AIP Applied Physics Letters

# AlGaN/GaN field effect transistors for power electronics—Effect of finite GaN layer thickness on thermal characteristics

C. Hodges, J. Anaya Calvo, S. Stoffels, D. Marcon, and M. Kuball

Citation: Applied Physics Letters **103**, 202108 (2013); doi: 10.1063/1.4831688
View online: http://dx.doi.org/10.1063/1.4831688
View Table of Contents: http://scitation.aip.org/content/aip/journal/apl/103/20?ver=pdfcov
Published by the AIP Publishing

# AlGaN/GaN field effect transistors for power electronics—Effect of finite GaN layer thickness on thermal characteristics

C. Hodges,[1,a)] J. Anaya Calvo,[1] S. Stoffels,[2] D. Marcon,[2] and M. Kuball[1]
[1]*H. H. Wills Physics Laboratory, University of Bristol, Bristol BS8 1TL, United Kingdom*
[2]*IMEC, Kapeldreef 75, B3001 Leuven, Belgium*

(Received 1 October 2013; accepted 1 November 2013; published online 12 November 2013)

AlGaN/GaN heterostructure field effect transistors with a 150 nm thick GaN channel within stacked $Al_xGa_{1-x}N$ layers were investigated using Raman thermography. By fitting a thermal simulation to the measured temperatures, the thermal conductivity of the GaN channel was determined to be 60 W $m^{-1}$ $K^{-1}$, over 50% less than typical GaN epilayers, causing an increased peak channel temperature. This agrees with a nanoscale model. A low thermal conductivity AlGaN buffer means the GaN spreads heat; its properties are important for device thermal characteristics. When designing power devices with thin GaN layers, as well as electrical considerations, the reduced channel thermal conductivity must be considered. © *2013 AIP Publishing LLC*. [http://dx.doi.org/10.1063/1.4831688]

AlGaN/GaN high electron mobility transistors (HEMTs) offer great promise for high-efficiency power conversion applications at higher voltages and temperatures than current technologies enable. This developing technology, however, still faces reliability issues. It is known that some of the degradation mechanisms[1] have a significant thermal acceleration component. Being able to accurately monitor and optimize the temperature of an operating heterostructure, field effect transistor (HFET) is therefore essential. AlGaN/GaN/AlGaN double HFETs (DHFETs) have been used for power applications,[2] enabling high breakdown voltages important for switching converters. However, the implications of using a thin GaN device channel on thermal performance have not been studied to date. It is known that thin (up to hundreds of nanometers) semiconductor layers generally have reduced thermal conductivity compared to the bulk material as studied for Si and SiGe;[3,4] this effect has not been considered yet for GaN, in particular in a device context. The thermal conductivity of the GaN channel is of particular importance in a DHFET, as it should act as a heat spreader layer when on top of an AlGaN buffer, which inherently has a much lower thermal conductivity than GaN,[5] by an order of magnitude. In this work, the thermal conductivity of a 150 nm thin GaN channel in an AlGaN/GaN DHFET was found to be around 60 W $m^{-1}$ $K^{-1}$, a reduction of more than 50% compared to typical GaN epilayers, leading to significantly increased channel temperatures in AlGaN/GaN/AlGaN DHFETs and the implications on the device thermal characteristics were studied.

The AlGaN/GaN/AlGaN DHFETs on Si substrates studied here consisted of a 150 nm GaN channel layer on top of multiple $Al_xGa_{1-x}N$ layers, with the aluminum fraction x decreasing in steps from the substrate to the device channel, with a 7 nm $Al_{0.45}Ga_{0.55}N$ barrier layer on top of the GaN channel (Figure 1). The source–drain spacing was 11.5 $\mu$m with a 1.5 $\mu$m gate and a gate–drain spacing of 8 $\mu$m. The ohmic contacts were TiAlMoAu, and the Schottky gate was Ni/Au. The gate contact was a T-gate with an overhang of 1 $\mu$m towards the drain. The devices were operated up to $V_{DS} = 20$ V. The source-gate pinch-off voltage was +475 mV. Enhancement mode operation was achieved by selective removal of *in-situ*-grown SiN before gate deposition. More details on the devices can be found in Ref. 6.

Raman thermography is a useful tool for extracting the channel temperature of electronic devices with submicron spatial resolution.[7–9] For the Raman thermography measurements, a Raman spectrometer operating at 532 nm in backscatter configuration was used. The devices were scanned under the laser spot in 0.25 $\mu$m steps, to record temperature profiles. The laser spot size was 0.5 $\mu$m. The temperature of a given layer of the device was determined from the shift of the corresponding Raman peak from a reference spectrum recorded with the device pinched off, as is commonly used to consider the effects of strain.[7] A typical Raman spectrum of the device studied here is shown in Figure 2. Each of the device layers, with its Al fraction, is apparent in the Raman spectrum. The frequencies of the modes observed are compatible with those reported in the literature, for example in Ref. 10. The $A_1$ phonon mode was used where possible to determine the device temperature (for the GaN and $Al_{0.70}Ga_{0.30}N$ it was necessary to use the $E_2$ line for

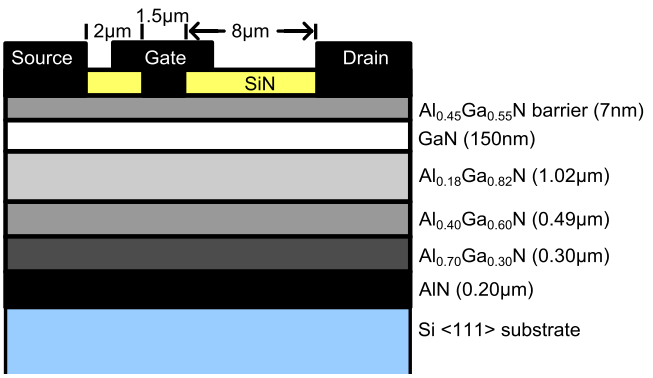


FIG. 1. Schematic of AlGaN/GaN DHFET structure studied.

a)Electronic mail: chris.hodges@bristol.ac.uk

 

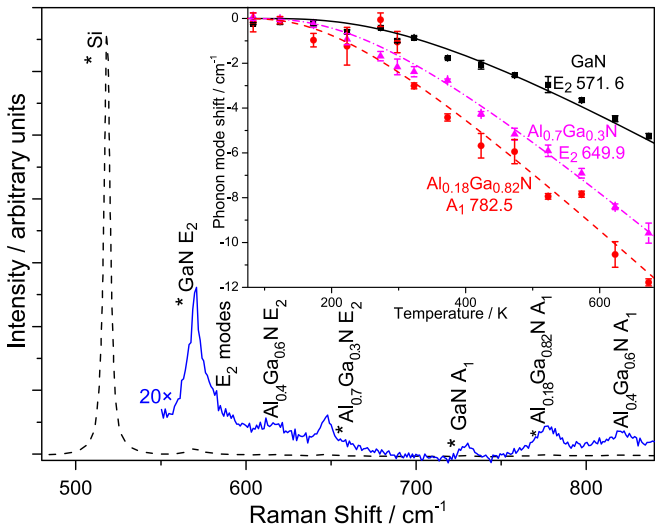


FIG. 2. Typical Raman spectrum of the DHFET studied. Asterisks indicate peaks used in the Raman thermography measurements. The inset shows experimental and fitted temperature-dependent phonon mode shifts with respect to the phonon frequency at 0 K, obtained by background heating/cooling of the device for the calibration measurement.

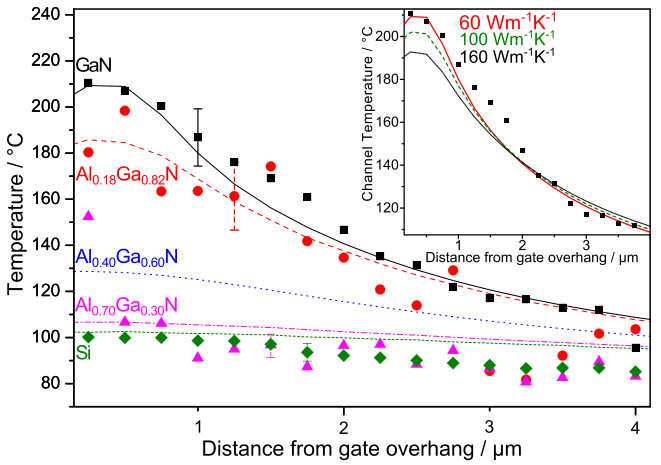


FIG. 3. Experimental (points) and simulated (lines) temperature distribution of an AlGaN/GaN DHFET across the gate-drain access region, with the device operated at $V_{DS} = 20$ V, $V_{GS} = 1$ V ($I_D = 325$ mA mm$^{-1}$), at 6.5 Wmm$^{-1}$ with a backplate temperature of 25 °C. The inset shows the simulated temperature of the GaN channel for a range of GaN thermal conductivities considering for typical GaN epilayers a thermal conductivity of 160 W m$^{-1}$ K$^{-1}$. Representative error bars are shown.

improved signal-to-noise ratio in the temperature measurement). For $Al_xGa_{1-x}N$, the $E_2$ mode splits into AlN-like and GaN-like lines, which share the intensity in approximate proportion to the Al fraction, for example, for $Al_{0.18}Ga_{0.82}N$ the GaN-like mode is much stronger than the AlN-like mode, which is even not observable, and correspondingly for the other layers. Broadening for $Al_xGa_{1-x}N$ Raman modes due to alloy disorder is observed for both $E_2$ and $A_1$, compatible with that reported by Davydov.[10] For calibration, thermal peak shifts for Raman-accessible phonon modes were determined as a function of temperature (inset to Figure 2) using backplate heating/cooling of the whole device. The thermal characteristics of the device were simulated in three dimensions using *Thermal Analysis System (TAS)* finite difference software from Ansys, Inc. As Raman thermography measures average temperature over each device layer thickness,[11] the temperature in the simulation was averaged over a volume corresponding to the laser focus within each layer when comparing to experimental data.

Figure 3 shows the temperature distribution in the AlGaN/GaN DHFET in the GaN channel and the different AlGaN layers in the gate-drain access region of the device, with the device operated at 6.5 Wmm$^{-1}$. The temperature peaks near the drain side of the gate contact in the GaN channel. This is where the majority of the electrical power is dissipated as Joule heating in the device. Temperature decreases towards the Si substrate, as is apparent with each AlGaN layer closer to the Si substrate, with the heat sink of the device being at the back of the Si substrate. The higher noise in the measured temperature data for the $Al_xGa_{1-x}N$ layers compared to the GaN and the Si substrate is due to the lower signal-to-noise for the corresponding Raman peaks (Figure 2). The presence of different compositions of $Al_xGa_{1-x}N$ provides the possibility to access three-dimensional thermal information of benefit when subsequently comparing experimental to thermal simulation data. The simulation assumed the majority of heat to be dissipated near the gate overhang as this provided the best agreement of the simulated to the experimental data.

Thermal simulations of the devices were performed using established thermal conductivity values for the $Al_xGa_{1-x}N$ layers from the literature.[12] The GaN thermal conductivity was fitted to give the best agreement to the experimental device data, in the device channel, and the different $Al_xGa_{1-x}N$ layers. A GaN thermal conductivity of 60 W m$^{-1}$ K$^{-1}$ was found to provide the best fit to the experimental data. This is more than 50% lower than the thermal conductivity of typical GaN epilayers, which is typically 160 W m$^{-1}$ K$^{-1}$.[13] The temperature profile was only weakly dependent on the thermal conductivities of the AlGaN buffer layers, though the thermal conductivity of the $Al_{0.18}Ga_{0.82}N$ did affect the magnitude of the temperature peak.

The inset to Figure 3 shows the dependence of peak channel temperature on GaN thermal conductivity in this device structure. The peak temperature in the channel is 20 °C higher when the GaN has a thermal conductivity of 60 W m$^{-1}$ K$^{-1}$ than if it had the typical GaN epilayer value of 160 W m$^{-1}$ K$^{-1}$. The inherently low thermal conductivity of the $Al_xGa_{1-x}N$ layers in the DHFET, typically of 20 W m$^{-1}$ K$^{-1}$, hinders optimal heat transport from the device channel to the substrate and therefore the heat sink. The thermal properties of the GaN channel are therefore critically important as it not only acts as the medium for transporting the electrons, but also as a heat spreader plate in the devices. In a nanolayer thinner than the bulk phonon mean free path, the cross-plane phonon transport is nearly ballistic, i.e., the phonons arrive at the boundary without suffering other scattering processes, then are scattered at the boundary. On the other hand, the lateral heat transport is severely limited by the proximity of the boundaries, which reduces the mean free path of the phonons inside the layer. The lateral thermal conductivity of the GaN is therefore of considerable importance to the peak channel temperature. This significant increase in peak channel temperature caused by the

decreased GaN thermal conductivity therefore exacerbates the effect of the low thermal conductivity $Al_xGa_{1-x}N$ stack on the device thermal characteristics.

To determine whether the reduced thermal conductivity of the 150 nm GaN layer in the DHFET of 60 W m$^{-1}$ K$^{-1}$ determined here is consistent with what is expected, a model considering thermal transport on the nanoscale was considered. In nanostructures, the mean free path of the phonons is comparable to the thickness $L$ of the layer,[14–16] as thermal transport is then dominated by the scattering events at the boundaries. In this regime one can approach the thermal transport through a phonon fluid in the Knudsen regime.[15,16] Using this formalism, the thermal conductivity of a thin film, $k_{\mathrm{Film}}$, can be expressed as a function of the bulk thermal conductivity $k_{\mathrm{B}}$,[17]

$$k_{\mathrm{Film}} = k_{\mathrm{B}} \frac{\Lambda_{\mathrm{eff}}}{\Lambda_{\mathrm{B}}} \tag{1}$$

introduced initially for Si, where $\Lambda_{\mathrm{B}}$ is the bulk mean free path of the phonons, and the effective phonon mean free path in the thin layer, $\Lambda_{\mathrm{eff}}$ is described as $(1/2)(\Lambda_1 + \Lambda_2)$, $\Lambda_1$ and $\Lambda_2$ being two functions of the Knudsen number $K_n = \Lambda_{\mathrm{B}}/L$ given by

$$\Lambda_1 = \Lambda_{\mathrm{B}} K_n \int_0^{\frac{1}{K_n}} \left( 1 + (\alpha - 1)\mathrm{e}^{-\alpha} - \alpha^2 \int_a^{\infty} \beta^{-1}\mathrm{e}^{-\beta}\mathrm{d}\beta \right) \mathrm{d}\alpha$$

$$\Lambda_2 = \Lambda_{\mathrm{B}} \left( 1 - \left( \frac{1}{K_n} - 1 \right) \mathrm{e}^{\frac{1}{K_n}} - \left( \frac{1}{K_n} \right)^2 \int_{\frac{1}{K_n}}^{\infty} \beta^{-1}\mathrm{e}^{-\beta}\mathrm{d}\beta \right). \tag{2}$$

The mean free path of phonons for GaN ($\Lambda_{\mathrm{B}}$) can be obtained from the classical kinetic expression for the thermal conductivity as $k = (1/3)C_v\Lambda_{\mathrm{B}}v$, which relates the thermal conductivity $k$ to the heat capacity $C_v$ and the sound velocity $v$, using $C_V \sim 35$ J mol$^{-1}$ K$^{-1}$ at 300 K,[18] while values ranging from 3338 m s$^{-1}$ to 5000 m s$^{-1}$ were reported for the sound velocities of GaN.[18–20] Taking into account that the accepted value for the thermal conductivity of the GaN epilayer used in typical GaN devices is ~160 W m$^{-1}$ K$^{-1}$, the mean free path of phonons calculated through the kinetic expression for GaN is 278 nm and 410 nm using the lower and higher sound velocities, respectively. Introducing these values for $\Lambda_{\mathrm{B}}$ into Eq. (1), the thermal conductivity for a layer with a thickness of 150 nm is within the range 62–78 W m$^{-1}$ K$^{-1}$, in excellent agreement with our experimental value of 60 W m$^{-1}$ K$^{-1}$. Figure 4 illustrates the thermal conductivity of the GaN as a function of the layer thickness determined using these mean free paths. It is apparent that for device GaN layer thickness in the 10 s of nanometers, the thermal conductivity will be in the region of 15–25 W m$^{-1}$ K$^{-1}$, comparable to AlGaN, and therefore the GaN channel will no longer provide a heat spreading function in the devices.

In conclusion, the thermal conductivity of a 150 nm GaN channel layer in an AlGaN/GaN/AlGaN DHFET was found by Raman thermography and simulation to be ~60 W m$^{-1}$ K$^{-1}$, significantly less than that of a typical GaN epilayer. Due to the low thermal conductivity of the AlGaN device layers, the GaN acts as a heat spreader in the devices. This thermal benefit of the GaN channel layer, however, disappears when its thickness is reduced to the 10 s of nanometers range. The resulting increased peak channel temperature has implications which need to be considered for optimizing AlGaN/GaN/AlGaN DHFET designs. The ability to measure the temperature of $Al_xGa_{1-x}N$ buffer and interface layers within an operating AlGaN/GaN/AlGaN DHFETs was demonstrated, in addition to directly measuring the temperature of the GaN device channel itself.

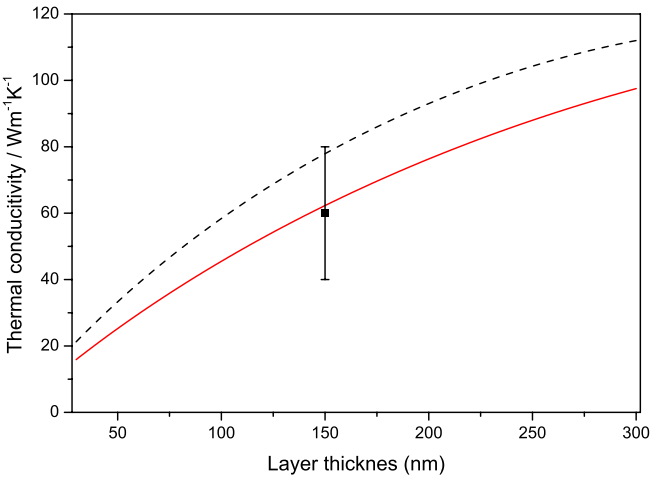


FIG. 4. GaN thermal conductivity at room temperature determined using the nanoscale model as a function of layer thickness considering sound velocities of 3338 m s$^{-1}$ (solid red line) and 5000 m s$^{-1}$ (dashed black line), and comparison to the experimental value determined here.

This work was in part supported by the Engineering and Physical Sciences Research Council (EPSRC).

[1]E. Zanoni, G. Meneghesso, M. Meneghini, A. Stocco, F. Rampazzo, R. Silvestri, I. Rossetto, and N. Ronchi, ECS Trans. **41**, 237 (2011).
[2]B. De Jaeger, M. Van Hove, D. Wellekens, X. Kang, H. Liang, G. Mannaert, K. Geens, and S. Decoutere, in *24th International Symposium on Power Semiconductor Devices and ICs (ISPSD)* (2012), pp. 49–52.
[3]J. Anaya, J. Jiménez, and T. Rodríguez, in *Nanowires–Recent Advances*, edited by X. Peng (InTech, 2012).
[4]Y. Zhao, C. Zhu, S. Wang, J. Z. Tian, D. J. Yang, C. K. Chen, H. Cheng, and P. Hing, J. Appl. Phys. **96**, 4563 (2004).
[5]B. C. Daly, H. J. Maris, A. V. Nurmikko, M. Kuball, and J. Han, J. Appl. Phys. **92**, 3820 (2002).
[6]J. Derluyn, M. Van Hove, D. Visalli, A. Lorenz, D. Marcon, P. Srivastava, K. Geens, B. Sijmus, J. Viaene, X. Kang, J. Das, F. Medjdoub, K. Cheng, S. Degroote, M. Leys, G. Borghs, and M. Germain, in *2009 IEEE International Electron Devices Meeting (IEDM)* (2009), pp. 1–4.
[7]M. Kuball, J. M. Hayes, M. Uren, T. Martin, J. C. H. Birbeck, R. Balmer, and B. Hughes, IEEE Electron Device Lett. **23**, 7 (2002).
[8]N. Killat, M. Kuball, T. Chou, U. Chowdhury, and J. Jimenez, in *2010 IEEE International Reliability Physics Symposium (IRPS)* (2010), pp. 528–531.
[9]T. Batten, J. W. Pomeroy, M. J. Uren, T. Martin, and M. Kuball, J. Appl. Phys. **106**, 094509 (2009).
[10]V. Y. Davydov, I. N. Goncharuk, A. N. Smirnov, A. E. Nikolaev, W. V. Lundin, A. S. Usikov, A. A. Klochikhin, J. Aderhold, J. Graul, O. Semchinova, and H. Harima, Phys. Rev. B **65**, 125203 (2002).
[11]A. Sarua, H. Ji, K. Hilton, D. Wallis, M. Uren, T. Martin, and M. Kuball, IEEE Trans. Electron Devices **54**, 3152 (2007).
[12]W. Liu and A. A. Balandin, Appl. Phys. Lett. **85**, 5230 (2004).
[13]M. Kuball, G. Riedel, J. Pomeroy, A. Sarua, M. Uren, T. Martin, K. Hilton, J. Maclean, and D. Wallis, IEEE Electron Device Lett. **28**, 86 (2007).

[14]E. Ziambaras and P. Hyldgaard, Mater. Sci. Eng., C **25**, 635 (2005).
[15]E. Ziambaras and P. Hyldgaard, J. Appl. Phys. **99**, 054303 (2006).
[16]Y. Ma, Appl. Phys. Lett. **101**, 211905 (2012).
[17]G. H. Tang, Y. Zhao, G. X. Zhai, and C. Bi, J. Appl. Phys. **110**, 046102 (2011).
[18]B. A. Danilchenko, T. Paszkiewicz, S. Wolski, A. Jeżowski, and T. Plackowski, Appl. Phys. Lett. **89**, 061901 (2006).
[19]J. Zou, D. Kotchetkov, A. A. Balandin, D. I. Florescu, and F. H. Pollak, J. Appl. Phys. **92**, 2534 (2002).
[20]D. T. Morelli, J. P. Heremans, and G. A. Slack, Phys. Rev. B **66**, 195304 (2002).